JOURNAL OF SOLID STATE CHEMISTRY 77, 132–140 (1988)

Lithium Ferrite Formation by Precipitation from Fe(III) Solutions

C. BARRIGA

Departamento de Química Inorgánica e Ingeniería Química, Facultad de Ciencias, Universidad de Córdoba, 14004 Córdoba, Spain

V. BARRON

Departamento de Edafología, Escuela Técnica Superior de Ingenieros Agrónomos, Universidad de Córdoba, 14004 Córdoba, Spain

R. GANCEDO AND M. GRACIA

Instituto de Química Física "Rocasolano", Consejo Superior de Investigaciones Científicas, Madrid

J. MORALES* AND J. L. TIRADO

Departamento de Química Inorgánica e Ingeniería Química, Facultad de Ciencias, Universidad de Córdoba, 14004 Córdoba, Spain

AND J. TORRENT

Departamento de Edafología, Escuela Técnica Superior de Ingenieros Agrónomos, Universidad de Córdoba, 14004 Córdoba, Spain

Received March 28, 1988; in revised form June 30, 1988

The formation of a new lithium ferrite modification structurally similar to γ-Fe_2O_3 and $LiFe_5O_8$ by direct precipitation from Fe(III) solutions is described. It is used as intermediate in the preparation of other lithium ferrites and contains no Fe(II) as revealed by Mössbauer spectroscopy and chemical analysis. Thermogravimetric results show a complex water loss at 80–500°C yielding a solid solution of γ-Fe_2O_3 and $LiFe_5O_8$ that decomposed to $LiFe_5O_8$ and α-Fe_2O_3 at 850°C. Hydrothermal treatment of the initial gel at 160°C leads to the progressive formation of α, β, and γ-$LiFeO_2$.

Introduction

Lithium ferrites, $LiFe_5O_8$ and $LiFeO_2$, are prepared by calcination of fine powder mixtures of Li_2CO_3 and Fe_2O_3 (*1–3*) or by crystallization from Li_2O–B_2O_3–Fe_2O_3 melts (*4, 5*). Recently, the lithiation products of Fe_2O_3 and Fe_3O_4 were prepared by chemical reaction of the oxides with *n*-butyl lithium (*6*). Divalent metal ferrites MFe_2O_4 (M = Fe, Mn, Co, Ni, Mg) can be obtained by the air oxidation of aqueous suspensions

* To whom correspondence should be addressed.

0022-4596/88 $3.00

of FeOOH and $M(OH)_2$ (*7–9*). In contrast, the preparation of lithium ferrites by wet procedures is less frequent (*10*). Recently (*11*), the ordered form β-$LiFe_5O_8$ was obtained by the reaction of Li with alkaline suspensions of iron(III) hydroxide. Similarly, γ-Fe_2O_3 is prepared by thermal (*12–14*) or mechanochemical (*15*) decomposition of γ-FeOOH or by oxidation of Fe_3O_4 (*16, 17*), while the corindon-structure phase α-Fe_2O_3 can be obtained by precipitation reactions.

In the present paper, we study the direct precipitation of a new lithium ferrite modification structurally similar to γ-Fe_2O_3 and $LiFe_5O_8$. The effect of thermal and hydrothermal treatments of this phase is also studied. These treatments allow the formation of known phases of the Li–Fe–O system without the high temperatures required in the ceramic method.

Experimental

All the chemicals used, $Fe(NO_3)_3$, LiOH, $LiNO_3$, and NaOH, were of analytical grade (Merck). Distilled water was used for the preparation of chemical solutions.

In order to study the effect of Li^+ and total OH^- concentration on the composition and structure of the phases obtained by the direct precipitation procedure, several experiments were performed with LiOH/NaOH solutions of variable concentration. The volume was fixed to 100 ml and the reaction temperature was 90°C. The products were washed with ammonium oxalate buffer solution of pH 3 to eliminate possible ferric gels. They were also repeatedly washed with water until the water was free from Li^+ ions. Total Fe and Li contents were determined with an atomic absorption spectrometer (Perkin–Elmer Model 302). The Fe(II) contents were determined by the *o*-phenantroline method.

Thermal analysis of the precipitates was performed on a simultaneous TG and DTA Stanton Redcroft apparatus Model STA 781.

The hydrothermal transformation of the original gel was carried out with a laboratory autoclave (Phaxe 2005).

The different products were examined by X-ray diffraction, Mössbauer spectroscopy, and electron microscopy. The 2θ angles of the diffraction peaks were calibrated against a standard Si powder by using Fe-filtered Co$K\alpha$ radiation or Ni-filtered Cu$K\alpha$ radiation. The size of the coherently diffracting domains and the content of microstrains was estimated by profile fitting to Pearson-VII functions (*18*). The electron micrographs and electron diffractograms were obtained with a JEOL 200CX microscope with side-entry stage. Transmission Mössbauer spectra of powder samples were recorded at RT, 77 K, and 14 K in a conventional constant acceleration spectrometer equipped with a ^{57}Co/Pd source and a helium closed-cycle cryostat. Spectra were computer fitted to Lorentzian lines using the alternative version to fit sextets of Stone's program (*19*).

Results

The phases identified in the course of several experiments carried out under different experimental conditions are included in Fig. 1, which visualizes the influence of Li^+, Na^+, and OH^- concentrations in the nature of the final product. The aging period of all precipitates was fixed to 7 days, since the degree of crystallinity remains almost unaltered after this period of time as will be discussed below. Low Li^+ concentration leads to the formation of iron oxyhydroxide (α-FeOOH) and/or α-Fe_2O_3 while high Li^+ and low OH^- concentrations lead also to similar phases. For Li^+ and OH^- concentrations greater than 1 and 2 *M*, respectively, a new phase structurally similar to γ-Fe_2O_3 and β-$LiFe_5O_8$ is obtained (see

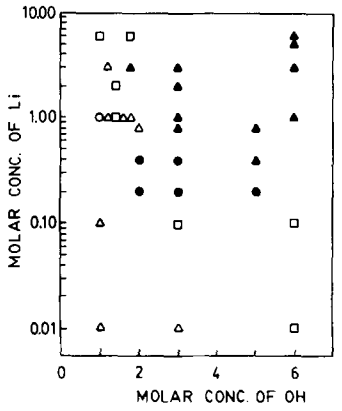

FIG. 1. Phase composition of the precipitates obtained with different Li and OH concentrations ($|OH^-| = |Li^+| + |Na^+|$): (○) α-Fe_2O_3, (△) α-Fe_2O_3 + α-FeOOH, (□) α-Fe_2O_3 + α-FeOOH + Intermediate, (●) α-FeOOH + Intermediate, (▲) Intermediate.

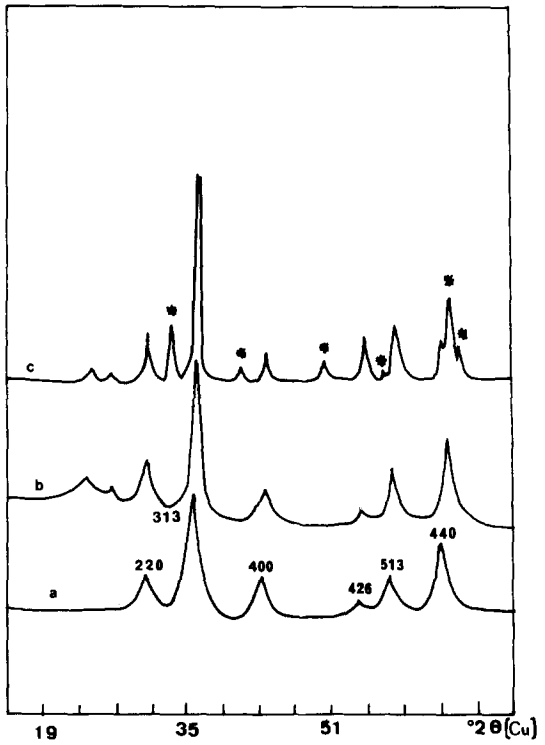

FIG. 2. XRD pattern of Intermediate (a) untreated, (b) heated to 700°C, and (c) heated to 850°C (*: α-Fe_2O_3).

Fig. 2a). Henceforth this phase will be referred to as Intermediate phase.

The crystallinity of the initial gel improves progressively with the aging time (Fig. 3). This results in a sharpening of the originally diffuse bands. After 7 days the Intermediate phase consists of aggregates of small particles (ca. 10 nm) which appear to be sheet-like morphology and flaky microstructure (Fig. 4). The observed mean size and particle shapes of the Intermediate phase obtained in all the concentration range were similar. On the other hand, Li concentration affects the degree of crystallization as reflected in Fig. 5. Higher Li^+ concentration and the increase in the precipitation temperature lead to a faster rate of crystallization as indicated by the plot of Fe_o/Fe_t ratio against aging time. The ratio Fe_o/Fe_t is, however, only a rough measurement of the degree of crystal growth, since the ammonium oxalate buffer solution can

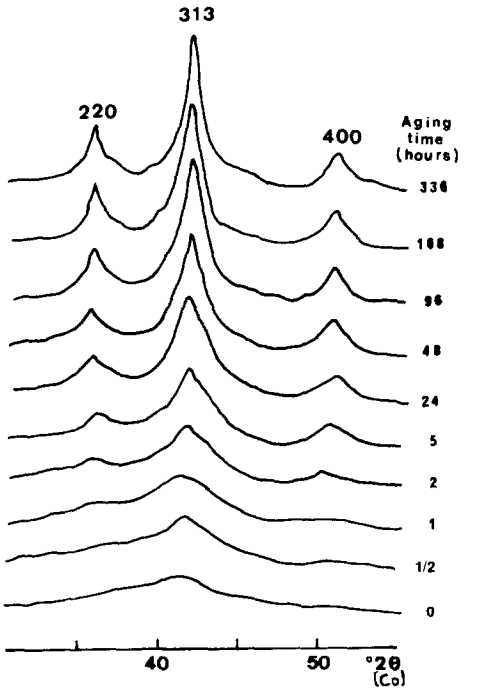

FIG. 3. XRD pattern evolution with aging time of the initial gel.

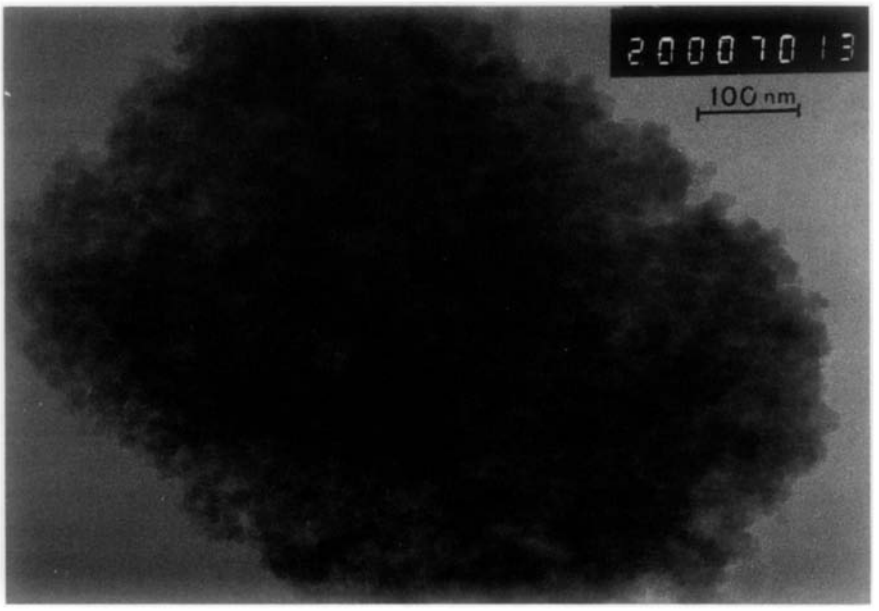

FIG. 4. Electron micrograph of the Intermediate.

partially disolve the Intermediate phase because of the small size of its particles (*20*).

The lattice constant of the Intermediate showed little variation with the preparation conditions; the mean value was 0.833 nm, close to the literature value for γ-Fe_2O_3 and $LiFe_5O_8$ (*4*, *21*). Chemical analysis of pure Intermediate showed a constant Li content (Li/Fe = 0.13_0). Neither Fe(II) nor Na was detected in the samples. It is noteworthy that this product was not identified in the preparation procedure used in (*11*). However, these authors indicate that for a low particle size it is possible to obtain a material with Li/Fe ratio lower than the unity that they ascribe to the presence of extremely fine superparamagnetic particles intermingled with ferromagnetic cubic particles of β-$LiFe_5O_8$.

The RT Mössbauer spectrum of the In-

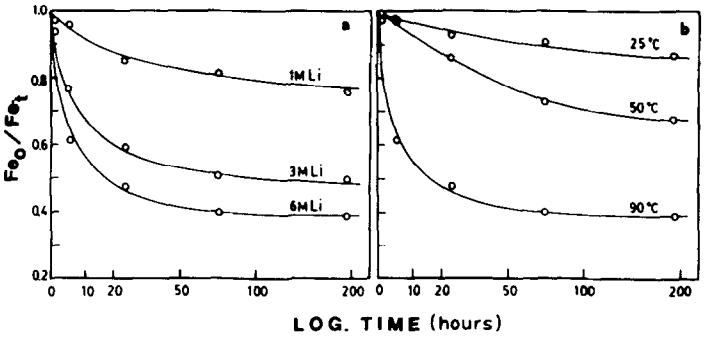

FIG. 5. Rate of crystallization of the initial gel for $|OH^-| = 6\ M$. (a) Effect of Li and (b) effect of the temperature for $|Li^+| = 6\ M$.

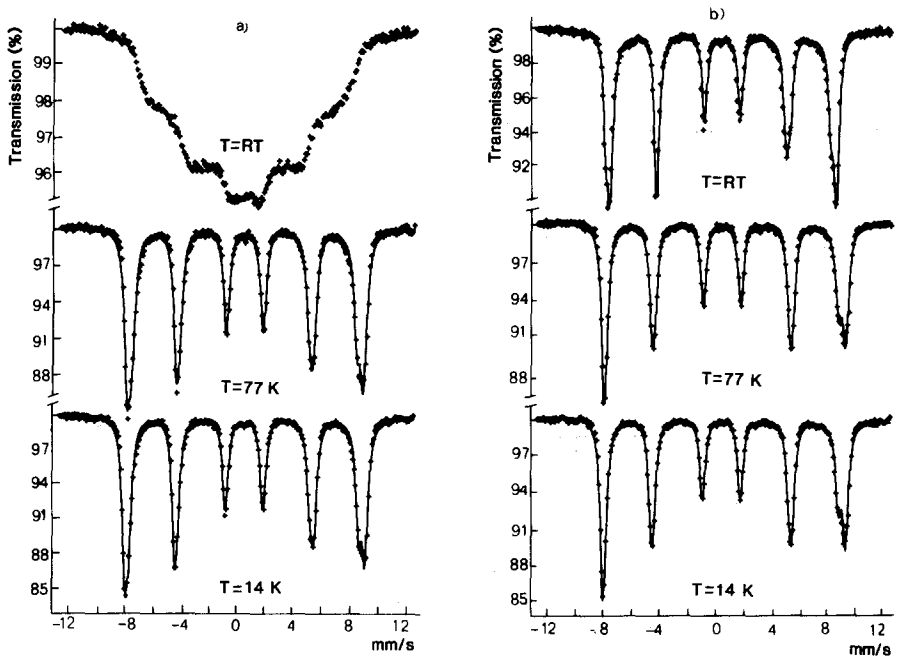

FIG. 6. Mössbauer spectra of the Intermediate phase (a) and the Intermediate after heating at 850°C (b).

termediate (Fig. 6a) yields very broad unresolved components characteristic of fine particles in the vicinity of the transition temperature. The maximum magnetic field calculated from the experimental spectrum is about 470 kG. The 77 and 14 K spectra of the Intermediate reveal at least two magnetic contributions, clearly reflected in the asymmetrical broadening of line 6 (Fig. 6a). The Mössbauer parameters obtained from the fitting to two sextets (Table I) indicate two different environments of Fe(III), which can be interpreted as octahedral (S_1) and tetrahedral (S_2) sites (*24–26*).

The thermal analysis curves of the Intermediate showed a complex weight loss in the temperature interval 80–500°C which can be due to water release, indicating the possible presence of hydroxyl groups or water molecules in the solid.

The thermal treatment of the Intermediate at 700°C leads to the formation of a hydrogen-free oxide with a composition in the range of the solid solutions of $LiFe_5O_8$ and γ-Fe_2O_3. The X-ray and electron diffraction data show that the particles have ordered vacancies in a tetragonal superstructure equivalent to that found in crystalline γ-Fe_2O_3 with $c = 3a$ (*22*).

The RT Mössbauer spectrum of the sample annealed at 700°C shows a magnetic sextet with broadened lines typical of a particle size distribution. Low-temperature spectra of this sample have a morphology similar to that of the unreacted Intermediate. Differences in linewidth and H (Table I) and between low-temperature spectra of the Intermediate and the product at 700°C are attributable to differences in particle or crystallite size (Table II).

At 850°C the solid solution decomposed to a mixture of two phases. Quantitative evaluation of X-ray diffractograms showed a composition of 67% of α-$LiFe_5O_8$ and

TABLE I

MÖSSBAUER PARAMETERS

Sample	Temp. (°K)	Sextet label	δ (mm · sec^{-1}) (±0.02)	Δ (mm · sec^{-1}) (±0.02)	H (kG) (±2)	Γ (mm · sec^{-1}) (±0.05)	I_{rel} (±0.04)
Interm.	RT		Unresolved components $H_{max} \simeq 470$ kG				
	77	S_1	0.39	0.05	527	0.53	0.57
		S_2	0.34	0.01	502	0.53	0.43
	14	S_1	0.40	0.06	536	0.49	0.58
		S_2	0.34	0.01	513	0.49	0.42
Interm. after heating at 700°C	RT		Magnetic distribution		440–500	—	—
	77	S_1	0.39	0.06	533	0.45	0.56
		S_2	0.32	−0.01	513	0.45	0.44
	14	S_1	0.40	0.06	537	0.43	0.58
		S_2	0.32	0.03	517	0.43	0.42
Interm. after heating at 850°C	RT	S_1	0.34	0.02	505	0.35[a]	0.32
		S_2	0.29	−0.01	489	0.48	0.39
		S_3	0.38	−0.13	518	0.35[a]	0.29
	77	S_1	0.50	0.21	539	0.51	0.58
		S_2	0.37	−0.03	522	0.51	0.42
	14	S_1	0.49	0.19	542	0.48	0.59
		S_2	0.37	−0.04	524	0.48	0.41

Note. δ, Isomer shift relative to α-Fe; Δ, quadrupole splitting; Γ, full-line width at half maximum; H, hyperfine magnetic field.

[a] Parameter value constrained in the fitting.

33% of γ-Fe_2O_3, in good agreement with the Li/Fe ratio of 0.12 found by atomic absorption spectrometry. Lithium sublimation reported for other lithium ferrites (*2*) was not detected. The electron diffraction data of this product supports the presence of the crystalline modification of $LiFe_5O_8$. The transformation takes place at a temperature considerably higher than that corresponding to the γ-$Fe_2O_3 \rightarrow \alpha$-$Fe_2O_3$ phase transition and is accompanied by a high recovery of the crystallinity of the solids, as shown by the values of the size of the coherently diffracting domains and microstrain content (Table II). This transformation is also characterized by a pronounced sintering process that results in an increase in particle size from 0.1 for the sample annealed at 700°C to 5 μm at 850°C.

An initial deconvolution of the RT spectrum of the product at 850°C (Fig. 6b) to two sextets yielded H values of 514 and 494 kG, respectively, but the χ^2/df (= 7) of the fitting was unacceptable. The fit to three sextets yielded the Mössbauer parameters listed in Table I with $\chi^2/df = 4$. The S_3 pa-

TABLE II

COMPOSITION AND STRUCTURAL PARAMETERS OF THE INTERMEDIATE AND ITS DECOMPOSITION PRODUCTS

Sample	Crystallite size (nm)	Microstrains	Li/Fe	a (nm)
Intermediate	11.5	0.0098	0.13_0	0.834_7
485°C	17.8	0.0001	0.13_4	0.833_9
700°C	27.2	0.0075	0.13_5	0.833_6
850°C	442.6	0.0030	0.13_0	0.832_4

rameter matches those corresponding to α-Fe_2O_3 (*27*), whereas those from S_1 and S_2 sextets are comparable to those of the Li Fe_5O_8 phase (*22, 24–26*). If equivalent recoil-free fractions for the three sextets are assumed, the hematite concentration can be obtained from the percentage of S_3 area in the spectrum. The obtained value of 29% is in acceptable agreement with the X-ray diffraction results. In the same way as the spectra of the Intermediate and the product of decomposition at 700°C, the 77 and 14 K spectra of samples decomposed at 850°C show asymmetry in the 1–6 lines and were fitted to two sextets (Fig. 6b). H values of S_1 and S_2 (Table I) are close to those of $LiFe_5O_8$ (*24–26*) but the quadrupole splitting Δ value of S_1 and the higher linewidth of both low-temperature subspectra in the product of decomposition at 850°C suggest the presence of a hematite phase (*28*). Attempts to fit both low-temperature spectra to three sextets did not improve the χ^2 and yielded an unusually high H value (550 kG) for one of the sextets. It is to be noted that in the low-temperature spectra of the Intermediate and the samples obtained by decomposition at 700 and 850°C the intensity ratio of S_2 to S_1 sextets is in the range 0.69–0.78 (Table I). The theoretical intensity ratio for γ-Fe_2O_3 is 0.60 for all vacancies in octahedral sites (*29, 30*).

Finally, hydrothermal treatment of the initial gel obtained in the presence of high Li^+ concentration (6 M) and Na^+ absence at 160°C leads to the formation of different modifications of $LiFeO_2$. When the aging time was 24 hr the product obtained was the disorder phase α-$LiFeO_2$, as shown in the X-ray diffraction pattern in Fig. 7a. From 24 to 336 hr of aging a progressive conversion of α-$LiFeO_2$ into the monoclinic (*33*) phase Q_{II} (β-$LiFeO_2$) takes place. From 336 to 912 hr the monoclinic Q_{II} phase transforms in the ordered Q_I (γ-$LiFeO_2$) phase. The X-ray diffraction pattern of this product (Fig. 7d) indexed in the tetragonal system leads to the unit cell parameters a = 0.408 and c = 0.865 nm, in good agreement with the literature values (*1, 32*).

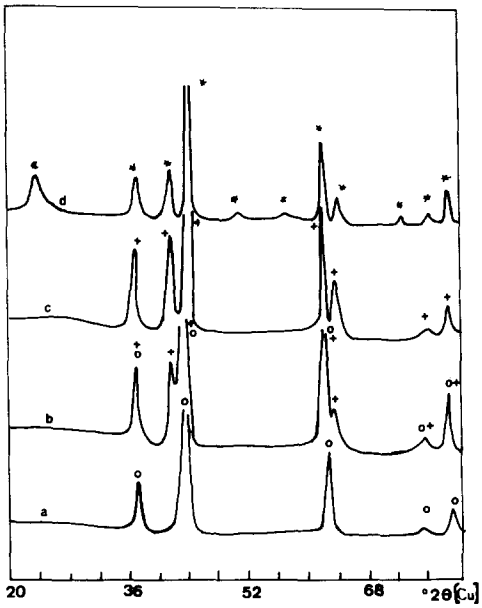

FIG. 7. XRD pattern of the product obtained by hydrothermal treatment at 160°C (a) 24 hr, (b) 120 hr, (c) 336 hr, (d) 912 hr. (○) α-$LiFeO_2$, (+) β-$LiFeO_2$, (*) γ-$LiFeO_2$.

Discussion

The Intermediate was identified as a monophasic lithiated solid with a structure similar to γ-Fe_2O_3, shown by the distribution of Fe(III) ions in tetrahedral and octahedral sites and a tetragonal superstructure with ordering of vacancies. This structure is not equivalent to β-$LiFe_5O_8$ which can be prepared by a similar procedure (*11*). Li is incorporated in the structure of the solid during Fe(III) precipitation for high OH^- concentrations. Under these conditions, α-Fe_2O_3 and α-FeOOH are not formed. However, the formation of the Intermediate by a wet procedure allows the simultaneous incorporation of hydrogen. This is evidenced by several types of water released in the TG experiment, which may include structurally

bound hydrogen. The introduction of H^+ and Li^+ ions in the structure without changing the formal III oxidation state of iron is possibly due to the structural similarities between γ-Fe_2O_3 and $LiFe_5O_8$ (*21, 23*) and the low size of H^+ and Li^+ ions. In fact, some authors proposed that γ-Fe_2O_3 may be a hydrogen iron oxide $H_{1-x}Fe_{5+x/3}O_8$ (*21*). The formation of the Intermediate in the presence of Li may allow the partial substitution of Li by H in a structure which is intermediate between γ-Fe_2O_3 and Li Fe_5O_8. Additionally, the Intermediate is stable as colloidal particles with high specific surface (185 m^2/g), favoring the external hydroxylation of the particles and the hydration of the final product.

On the other hand, the presence of Li and H in the structure of the solid favor a higher thermal stability of the Intermediate after losing the external water as compared with γ-Fe_2O_3 (*12*). However, the loss of the structural hydrogen leads to the formation of a solid solution in the $LiFe_5O_8$–Fe_2O_3 interval, namely, $Li_{0.62}Fe_{5.13}O_8$. This product is stable in a short temperature interval (730–800°C). Since the Li/Fe ratio is $\simeq$0.2, at higher temperatures, $LiFe_5O_8$ and the sesquioxide α-Fe_2O_3, which is a stable modification at the transformation temperature, are formed.

Although $LiFeO_2$ cannot be prepared by direct precipitation, the hydrothermal reaction of the initial gel used in the preparation of the Intermediate leads to the formation of $LiFeO_2$, whose crystalline structure depends markedly on the reaction time.

If we take into account the low temperature in which the hydrothermal treatment is carried out (160°C), it is noteworthy the short periods of time needed for the transformations between the various $LiFeO_2$ phases, as compared with time required by thermal treatment (*3, 31*). These results and the fact that the hydrothermal transformations proceed through a disorder (α) $\rightarrow$ order (β and γ) conversion may indicate that the phase transitions involve chemical transport in liquid and/or vapor phase. This effect increases ion mobility and consequently the rate of conversion.

On the other hand, the sequence of transformations under hydrothermal conditions $\alpha \rightarrow \beta \rightarrow \gamma$ is in agreement with that proposed by Anderson and Schieber (*1*) in which β-$LiFeO_2$ is suggested as an intermediate phase during the ordering process.

Acknowledgment

The authors thank the Spanish CAICYT for financial support of this work, which was carried out at the Department of Inorganic Chemistry of Córdoba under Project 0982-84.

References

1. J. C. Anderson and M. Schieber, *J. Phys. Chem. Solids* **25,** 88 (1964).
2. M. Amemiya, *J. Inorg. Nucl. Chem.* **34,** 3405 (1972).
3. N. Ramachandran and A. B. Biswas, *J. Solid State Chem.* **30,** 61 (1979).
4. M. Schieber, *J. Inorg. Nucl. Chem.* **26,** 1363 (1964).
5. C. Chaumont and J. C., Bernier, *J. Solid State Chem.* **38,** 246 (1981).
6. M. M. Thackeray, W. I. F. David, and J. J. Goodenough, *Mater. Res. Bull.* **17,** 785 (1982).
7. M. Kiyama, *Bull. Chem. Soc. Japan* **51,** 134 (1978).
8. Y. Tamaura, P. V. Buduan, and T. Katsura, *J. Chem. Soc. Dalton Trans.,* 1807 (1981).
9. Y. Tamaura, *Inorg. Chem.* **24,** 4363 (1985).
10. M. Kiyama and T. Takada, *Bull. Inst. Chem. Res. Kyoto Univ.* **58,** 193 (1980).
11. M. Kiyama, T. Kurata, and T. Takada, *Bull. Chem. Soc. Japan* **60,** 3931 (1987).
12. R. C. Mackenzie and G. Berggren, "Differential Thermal Analysis," Academic Press, New York (1970).
13. K. Bechine, J. Subrt, T. Hanslik, V. Zapetal, J. Tlaskal, J. Lipka, B. Sedlak, and M. Rotter, *Z. Anorg. Allg. Chem.* **489,** 186 (1982).
14. R. Gomez-Villacieros, L. Hernan, J. Morales, and J. L. Tirado, *J. Colloid Interface Sci.* **101,** 392 (1984).
15. R. Gomez-Villacieros, J. Morales, and J. L. Tirado, *J. Chem. Soc. Chem. Commun.,* 559 (1984).

16. F. FEITKNECHT, *Pure Appl. Chem.* **9,** 423 (1964).
17. B. GUILLOT, A. ROUSSET, AND G. DUPRE, *J. Solid State Chem.* **25,** 263 (1978).
18. TH. H. DE KEIJSER, E. MITTEMEIJER, AND H. C. R. ROZENDAAL, *J. Appl. Crystallogr.* **16,** 309 (1983).
19. A. J. STONE, H. J. AAGAARD, AND J. FENGER, *Riso Rep.*, M-1348 (1974).
20. V. SCHWERTMANN, *Z. Pflanzenernaehr. Dueng. Bodenkd.* **105,** 194 (1964).
21. P. B. BRAUN, *Nature (London)* **27,** 1123 (1952).
22. K. HANEDA AND A. H. MORRISH, *Solid State Commun.* **22,** 779 (1977).
23. C. GREAVES, *J. Solid State Chem.* **49,** 325 (1983).
24. B. LEREBOURS AND M. LENGLET, *Ann. Chim. Fr.* **4,** 347 (1979).
25. N. K. GILL AND R. K. PURI, *Spectrochim. Acta A* **41,** 1005 (1985).
26. F. S. BARROS, P. J. VICCARO, AND J. O. ARTMAN, *Phys. Lett. A* **27,** 374 (1968).
27. L. H. BOWEN, *Mössbauer Eff. Ref. Data J.* **2,** 76 (1979).
28. A. E. VERBEECK, E. DE GRAVE, AND R. E. VANDENBERGHE, *Hyperfine Interact.* **28,** 639 (1986).
29. R. J. ARMSTRONG, A. H. MORRISH, AND G. A. SAWATZKY, *Phys. Lett.* **23,** 414 (1966).
30. K. HANEDA AND A. H. MORRISH, *Phys. Lett. A* **64,** 259 (1977).
31. D. COX, P. A. SHIRANE, P. A. FLINN, S. L. RUBY, AND W. J. TAKEI, *Phys. Rev.* **132,** 1547 (1963).
32. M. FAYARD, *Ann. Chim.* **6,** 1279 (1961).
33. R. FAMERY, P. BASSOUL, AND F. QUEYROUX, *J. Solid State Chem.* **57,** 178 (1985).